Available online at www.sciencedirect.com

SciVerse ScienceDirect

Scripta Materialia 67 (2012) 760–762

Scripta MATERIALIA

www.elsevier.com/locate/scriptamat

Surface energies of AlN allotropes from first principles

David Holec* and Paul H. Mayrhofer

Montanuniversität Leoben, Franz-Josef-Straße 18, Leoben A-8700, Austria

Christian Doppler Laboratory for Application Oriented Coating Development at the Department of Physical Metallurgy and Materials Testing, Montanuniversitt Leoben, Franz-Josef-Straße 18, Leoben A-8700, Austria

Received 26 June 2012; revised 18 July 2012; accepted 19 July 2012

Available online 27 July 2012

In this letter we present first-principles calculations of the surface energies of rock-salt (B1), zinc-blende (B3) and wurtzite (B4) AlN allotropes. Of several low-index facets, the highest energies are obtained for monoatomic surfaces (i.e. of only either Al or N atoms): $\gamma^{B1}_{\{111\}} = 410\ \mathrm{meV/Å^2}$, $\gamma^{B3}_{\{100\}} = 346\ \mathrm{meV/Å^2}$, $\gamma^{B3}_{\{111\}} = 360\ \mathrm{meV/Å^2}$ and $\gamma^{B4}_{\{0001\}} = 365\ \mathrm{meV/Å^2}$. The difference between Al- and N-terminated surfaces in these cases is less then $20\ \mathrm{meV/Å^2}$. The stoichiometric facets have energies lower by $100\ \mathrm{meV/Å^2}$ or more. The obtained trends could be rationalized by a simple nearest-neighbour broken-bond model.

Keywords: Aluminium nitride; Surface energy; Density functional theory; Broken-bond model

Aluminium nitride is a material used in a wide variety of applications, spanning from optoelectronic [1] and acoustic [2] devices to the beneficial influence on mechanical properties (e.g. increased hardness) and performance of protective hard coatings [3]. It crystallizes in the wurtzite structure (B4, space group $P6_3mc$). Under non-equilibrium deposition parameters, its metastable zinc-blende variant (B3, space group $F\bar{4}3m$) can be stabilized [4]. Finally, under pressures above ≈16 GPa [5] it transforms to the rock-salt structure (B1, space group $Fm\bar{3}m$).

Knowledge of surface energies and the corresponding trends is important in several areas. As discussed by Gall et al. [6] for the case of TiN, surface energy is a decisive parameter for the thin film microstructure when grown under near-to-equilibrium conditions, i.e. when thermodynamics rather than kinetics control the texture formation. This is the case, for example, of the chemical vapour deposition of AlN for optoelectronic applications. It is equally important in the discussion of decomposition pathways of, for example, unstable $Ti_{1-x}Al_xN$ [7,8]. Another emerging area of interest is the stabilization of rock-salt AlN using a multilayer architecture for $Ti_{1-x}Al_xN$/AlN or $Cr_{1-x}Al_xN$/AlN coatings [9], as it strengthens the material and has the potential to stop and/or deflect cracks [10]. Due to the nanostructured character of these composites, surface energy makes a non-negligible contribution to the overall energetic balance [11].

Although many papers have been published both on calculations and on experimental results, a systematic study of the surface energies has yet to be reported. In this letter we use quantum mechanical calculations to obtain energies of several low-index clean surfaces (i.e. no surface reconstruction is considered here) of the B1, B3 and B4 allotropes. Since we cover several surface orientations as well as crystallographic structures, these results represent a coherent data set which can be used directly in such as the above described applications.

Quantum mechanical calculations within the framework of density functional theory were performed using the Vienna Ab initio Simulation Package [12]. Projector-augmented wave method pseudopotentials used generalized gradient approximation [13] as parametrized by Perdew and Wang [14]. The first Brillouin zone (1BZ) of the bulk material unit cells was meshed with $5 \times 5 \times 5$, $8 \times 8 \times 8$ and $9 \times 9 \times 6$ k-points distributed according to the Monkhorst–Pack scheme for the B1, B3 and B4 allotropes, respectively. The sampling was adopted for the surface supercells (see below), with only one k-point along the direction perpendicular to the surface. The total energy was obtained by integration over the whole 1BZ using the tetrahedron method. These parameters, together with a plane wave cut-off energy of 450 eV, ensure an accuracy of the total energy of ≈1 meV atom^{-1}.

* Corresponding author. E-mail: david.holec@unileoben.ac.at

1359-6462
http://dx.doi.org/10.1016/j.scriptamat.2012.07.027

Table 1. Lattice constants a and c, total energy E_{tot} and energy of formation E_f of individual AlN structures (calculated and experimental lattice parameters from the literature are given for comparison).

	This study				Previous works			
	E_{tot} [eV/at.]	E_f [eV/at.]	a [Å]	c [Å]	a [Å]		c [Å]	
					Calc.	Expt.	Calc.	Expt.
B1	−7.3202	−1.3038	4.070		4.06 [15]	4.05 [16]		
B3	−7.4801	−1.4637	4.401		4.39 [15]	4.38 [4]		
B4	−7.5014	−1.4850	3.129	5.016	3.12 [15]	3.111 [17]	5.00 [15]	4.979 [17]

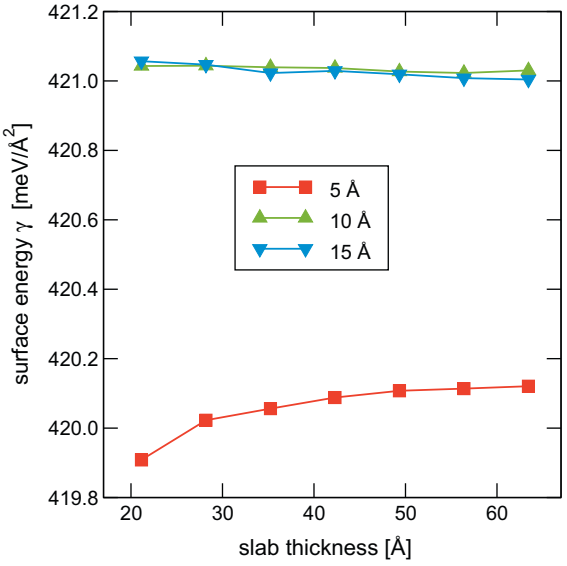

Figure 1. Convergence of the Al-terminated {111} surface energy of B1-AlN.

For each structure and each surface orientation, an N_{cell}-atom primitive cell was constructed such that the particular facet was perpendicular to the z-axis. Subsequently, n primitive cells were stacked along the z-axis followed by h_{vac} thick vacuum. Periodic boundary conditions were applied on those slabs. If the surface area is A and contains N_{surf} atoms, the surface energy is calculated as

$$\gamma(n, h_{vac}) = \frac{1}{2A}\left(E_{slab} - E_{bulk}(nN_{cell} + N_{surf})\right) \quad (1)$$

where E_{slab} is the total energy of the slab while E_{bulk} is the bulk total energy per atom of the respective structure. The positions of all atoms were relaxed during calculations of E_{slab}.

Finally, $\gamma(n, h_{vac})$ is converged simultaneously with respect to the number of primitive cells in the slab, n, and the vacuum thickness, h_{vac}, in order to rule out undesired surface interactions either through the bulk material or through the separating vacuum.

The calculated bulk lattice parameters (see Table 1) agree well with both the calculated and experimental values published previously. The lowest energy of formation is obtained for the wurtzite B4 structure, closely followed by the zinc-blende B3 ($\Delta E_f^{B3-B4} = 0.0213$ eV at.$^{-1}$). The rock-salt structure B1 possesses the highest energy of formation ($\Delta E_f^{B1-B4} = 0.1813$ eV at.$^{-1}$). These values correspond well with the data calculated by Siegel et al. [15].

In this study we consider four low-index surfaces ({100}, {110}, {111} and {112}) for the cubic B1 and B3 structures, and three different orientations

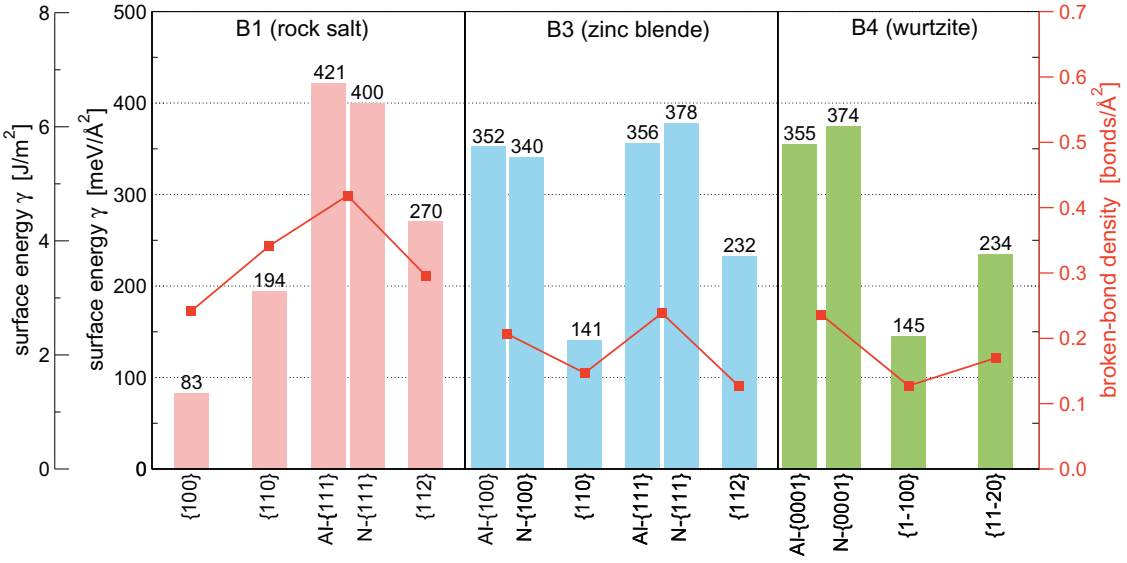

Figure 2. Surface energies for low-index planes of AlN allotropes. Red curves represent the calculated density of broken bonds, as discussed in the text. (For interpretation of the references to colour in this figure legend, the reader is referred to the web version of this article.)

($\{0001\}$, $\{1\bar{1}00\}$ and $\{11\bar{2}0\}$) for the hexagonal B4 phase. The respective primitive cells contain 4, 4, 6 and 12 atoms for the cubic structures and 4, 8 and 8 for the wurztite ones. Their exact description is given in the Supplementary material to this letter, available online. It is worth noting that the B1-$\{111\}$, B3-$\{100\}$, B3-$\{111\}$ and B4-$\{0001\}$ planes contain only atoms of one element. Consequently, in these cases we have calculated separately Al- and N-terminated surfaces.

A typical example of the surface energy as a function of the slab and vacuum thickness is shown in Figure 1 for the Al-terminated B1-$\{111\}$ surface. As in all other cases, the difference between results for 10 and 15 Å is negligible, while 5 Å gives different γ values. A slab thickness of ≈20 Å is sufficient in this case, but for other orientations thicker slabs are needed.

The resulting surface energies are shown in Figure 2. The highest values of γ (between 340 and 420 meV Å^{-2}) are for all structures obtained for single-element surfaces. Additionally, the difference between surfaces terminated with Al or N atoms are ≈20 meV or less. This means that in the cases when only the orientation rather than the exact structure of the surface is known, one can used the average value of Al- and N-terminated surfaces as a reasonable estimate without changing, for example, the energetic order of individual facets. The surface energy of facets formed by both atomic species (stoichiometric facets) is at least 100 meV Å^{-2} lower than the monoatomic ones. The lowest surface energies of individual structures possess $\{100\}$ planes for B1, $\{110\}$ planes for B3 and $\{1\bar{1}00\}$ planes for B4.

The observed trends can be rationalized by a simple nearest-neighbour broken-bond model [18,19]. If one assumes that the main contribution to the surface energy is the "penalty" related to breaking bonds that cross the actual surface, then γ should be proportional to N_{bonds}/A, where N_{bonds} is the number of broken bonds per surface area A of the primitive cell. This density of broken bonds is also plotted in Figure 2. The figure captures the surface energy trends surprisingly well, the only deficiencies being the mutual relations of the cubic $\{110\}$ and $\{112\}$ facets. Since no plane can cut more then three bonds of the octahedrally coordinated sites in the B1 structure (which is the case for $\{112\}$ plane), and since the surface area per atom increases for planes with higher Miller indices, the nearest-neighbour broken-bond model suggests that the surface energy of all those planes is less than $\gamma_{\{112\}} = 270$ meV Å^{-2}. The situation is slightly more complex for the octahedrally coordinated B3 and B4 structures. If a pair of mirror interfaces is always considered (as in the case of this study, where, for example, $\gamma^{\text{B4}}_{\{0001\}} = \frac{1}{2}(\gamma^{\text{B4}}_{(0001)} + \gamma^{\text{B4}}_{(000\bar{1})})$), then the maximum number of broken bonds per surface atom is two. The only possible way to get a surface with atoms having only one broken bond is that two out of four bonds lie on the surface. In all other cases, the surface atoms have two broken bonds per atom on average. Out of those, the B3-$\{111\}$ and B4-$\{0001\}$ planes have the smallest area per atom, thus accounting for $\gamma^{\text{B3}}_{\{111\}}$ and $\gamma^{\text{B4}}_{\{0001\}}$ having the highest surface energies of those structures.

Conclusions

We have used quantum mechanical calculations to obtain the surface energies of low-index surface facets of rock-salt B1, zinc-blende B3 and wurtzite B4 allotropes of AlN. No surface reconstruction was taken into account. The highest surface energies were obtained for single-element planes, i.e. $\gamma^{\text{B1}}_{\{111\}} = 410$ meV/Å^2, $\gamma^{\text{B3}}_{\{100\}} = 346$ meV/Å^2, $\gamma^{\text{B3}}_{\{111\}} = 360$ meV/Å^2 and $\gamma^{\text{B4}}_{\{0001\}} = 365$ meV/Å^2. The observed trends could be rationalized by the nearest-neighbour broken-bond model: the higher the areal density of broken bonds, the higher the surface energy.

Financial support from the Christian Doppler Research Association and from the START Program (Y371) of the Austrian Science Fund (FWF) is greatly acknowledged.

Appendix A. Supplementary data

Supplementary data associated with this article can be found, in the online version, at http://dx.doi.org/10.1016/j.scriptamat.2012.07.027.

[1] S.C. Jain, M. Willander, J. Narayan, R.V. Overstraeten, J. Appl. Phys. 87 (2000) 965.
[2] R. Turner, P. Fuierer, R. Newnham, T. Shrout, Appl. Acoust. 41 (1994) 299–324.
[3] P.H. Mayrhofer, A. Hörling, L. Karlsson, J. Sjölén, T. Larsson, C. Mitterer, L. Hultman, Appl. Phys. Lett. 83 (2003) 2049–2051.
[4] I. Petrov, E. Mojab, R.C. Powell, J.E. Greene, L. Hultman, J.-E. Sundgren, Appl. Phys. Lett. 60 (1992) 2491.
[5] D. Holec, F. Rovere, P.H. Mayrhofer, P.B. Barna, Scripta Mater. 62 (2010) 349–352.
[6] D. Gall, S. Kodambaka, M.A. Wall, I. Petrov, J.E. Greene, J. Appl. Phys. 93 (2003) 9086.
[7] P. Mayrhofer, F. Fischer, H. Böhm, C. Mitterer, J. Schneider, Acta Mater. 55 (2007) 1441–1446.
[8] R. Rachbauer, S. Massl, E. Stergar, D. Holec, D. Kiener, J. Keckes, J. Patscheider, M. Stiefel, H. Leitner, P.H. Mayrhofer, J. Appl. Phys. 110 (2011) 023515.
[9] V. Chawla, D. Holec, P.H. Mayrhofer, Comput. Mater. Sci. 55 (2012) 211–216.
[10] M. Schlögl, J. Paulitsch, J. Keckes, P.H. Mayrhofer, Surf. Coat. Technol., under review.
[11] V. Chawla, D. Holec, P.H. Mayrhofer, 2012.
[12] G. Kresse, J. Furthmüller, Phys. Rev. B 54 (1996) 11169–11186.
[13] G. Kresse, D. Joubert, Phys. Rev. B 59 (1999) 1758–1775.
[14] Y. Wang, J.P. Perdew, Phys. Rev. B 44 (1991) 13298–13307.
[15] A. Siegel, K. Parlinski, U. Wdowik, Phys. Rev. B 74 (2006) 104116.
[16] Powder Diffraction File 00-046-1200, International Center for Diffraction Data, PDF-2/Release 2007, 2007.
[17] O. Madelung, Semiconductors Data Handbook, vol. 8, Springer-Verlag, Berlin, 2004.
[18] E. Kozeschnik, I. Holzer, B. Sonderegger, J. Phase Equilib. Diffus. 28 (2007) 64–71.
[19] R. Becker, Ann. Phys. 424 (1938) 128–140.